DOI: 10.1002/cmdc.200800122

HER-2-Targeted Nanoparticle–Affibody Bioconjugates for Cancer Therapy

Frank Alexis,[a, b] Pamela Basto,[a, b] Etgar Levy-Nissenbaum,[a, b] Aleksandar F. Radovic-Moreno,[b] Liangfang Zhang,[b] Eric Pridgen,[c] Andrew Z. Wang,[b, d] Shawn L. Marein,[a] Katrina Westerhof,[a, b] Linda K. Molnar,[e] and Omid C. Farokhzad*[a, b]

Drug-encapsulated controlled release nanoparticles (NPs) have the potential to improve current cancer chemotherapies by increasing drug efficacy, lowering drug toxicity, and maintaining a relatively high concentration of drug at the site of interest.[1–3] Encapsulating drugs within NPs can improve the solubility and pharmacokinetics of drugs, and, in some cases, enable further clinical development of new chemical entities that have stalled because of poor pharmacokinetic properties. The breakthrough potential of cancer nanotechnology is becoming more apparent with several examples of untargeted NP platforms in current clinical use. These include Abraxane (paclitaxel–albumin),[4] Doxil (doxorubicin–liposomes),[5] DaunoXome (daunorubicin–liposomes),[6] Cyclosert (camptothecin–cyclodextrin),[7] and Genexol-PM [paclitaxel–methoxypoly(ethylene glycol)-poly(D,L-lactide)].[8] The functionalization of untargeted NPs with ligands that bind the extracellular domain of tumor-associated transmembrane antigens may further increase the therapeutic index of cytotoxic drugs by selectively targeting drugs to diseased cells.

The first examples of targeted NPs were reported in 1980, and despite nearly three decades of research, targeted NPs have made a limited impact on human health. This partially because the optimal bio-physicochemical properties of the NPs, including the choice of a suitable ligand for targeting, has remained elusive.[9–11] These include the use of targeting approaches that go beyond antibodies, which themselves have several drawbacks, including their large hydrodynamic size, which limits both intratumoral uptake and homogeneous distribution in the tumor, thus adversely affecting pharmacokinetic properties. Furthermore, the use of an antibody as a component of a multifunctional nanoparticle adds an additional level of complexity to the scale-up and manufacturing of the resulting targeted NPs. There is a clear need for new methods of targeting that are compatible with the size of NPs and their manufacture. Additionally, although monoclonal antibodies have shown some promise, their effects tend to be variable and ultimately not curative. Attempts to develop immunoconjugates, which add the therapeutic benefit of a drug, toxin, or radionuclide, have not met with much success either, and this is likely due to low drug content per antibody molecule. However, the combination of the targeting capacities of an antibody without the inherent limitations of antibodies[12] as mentioned above, and a controlled release system using a payload that consists of a small-molecule chemotherapeutic may prove advantageous.

The anti-[human epidermal growth factor receptor 2] (HER-2) affibody has many merits as a targeting ligand in contrast to an anti-HER-2 monoclonal antibody. Its small size ($M_r \sim 15$ kDa) results in a favorable ratio of binding site to ligand size, bearing in mind that the molecular weight of an anti-HER-2 monoclonal antibody is typically ~150 kDa; it promotes an endocytosis-dependent internalization mechanism;[13,14] it has a functional end group distanced from its active site for chemical conjugation; it has high in vitro and in vivo stability; and the total chemical synthesis allows facile, large-scale production. The anti-HER-2 affibody (Z-HER2: 342 affibody) has shown high binding affinity ($K_D \sim 22$ pM) to the recombinant extracellular domain of the HER-2 protein (HER-2-ECD).[15] In addition, Orlova et al.[15] have shown that this class of molecule can selectively bind to HER-2-overexpressing cell lines (SKBR-3 and SKOV-3). All of these characteristics make the affibody a potentially viable ligand for targeted drug delivery.

To develop HER-2-targeted drug-encapsulated NPs, we conjugated the anti-HER-2 affibody to the thiol-reactive maleimide group of the poly-(D,L-lactic acid)–poly(ethylene glycol)–maleimide (PLA-PEG-Mal) copolymer of the previously formed NPs through a stable thioether bond, and evaluated the targeting specificity and efficacy using fluorescence microscopy. We subsequently encapsulated paclitaxel into the targeted polymeric NPs and examined whether this system could increase the drug's cytotoxicity in two HER-2-positive cell lines: SKBR-3 and SKOV-3. We chose to deliver the taxane paclitaxel owing to its poor water solubility, which results in a decreased therapeutic index for intravenous administration of the free drug in a clinical setting.

We began with the synthesis of the PLA-PEG-Mal copolymer, which consists of a hydrophobic block [poly-(D,L-lactic acid)], a hydrophilic block [poly(ethylene glycol)], and a maleimide ter-

[a] Dr. F. Alexis, P. Basto, Dr. E. Levy-Nissenbaum, S. L. Marein, K. Westerhof, Prof. Dr. O. C. Farokhzad
Department of Anesthesiology
Brigham and Women's Hospital and Harvard Medical School
75 Francis St., Boston, MA 02115 (USA)
Fax: (+1) 617-730-2801
E-mail: ofarokhzad@partners.org

[b] Dr. F. Alexis, P. Basto, Dr. E. Levy-Nissenbaum, A. F. Radovic-Moreno, Dr. L. Zhang, Dr. A. Z. Wang, K. Westerhof, Prof. Dr. O. C. Farokhzad
Division of Health Science and Technology
Massachusetts Institute of Technology
77 Massachusetts Ave., Cambridge, MA 02139 (USA)

[c] E. Pridgen
Department of Chemical Engineering
Massachusetts Institute of Technology (USA)

[d] Dr. A. Z. Wang
Department of Radiation Oncology
Brigham and Women's Hospital and Harvard Medical School
75 Francis St., Boston, MA 02115 (USA)

[e] Dr. L. K. Molnar
National Cancer Institute
National Institutes of Health, Bethesda, Maryland, 20892 (USA)

Supporting information for this article is available on the WWW under http://dx.doi.org/10.1002/cmdc.200800122.

minal group. The copolymers then form negatively charged NPs with a core–shell structure in an aqueous environment through the nanoprecipitation method. The hydrophobic cores of the NPs are capable of carrying pharmaceuticals, especially those with poor water solubility. The hydrophilic shell provides not only a "stealth" layer,[16] which together with the surface charge property (ζ potential; $\zeta = -10 \pm 5$ mV)[17,18] improves the stability and circulation half-life of these drug-delivering NPs, but also functional maleimide groups for affibody conjugation (Figure 1 A). Lack of protein adsorption in solutions containing 10, 20, and 100% serum (data not shown) demonstrated the stability of NP size (< 100 nm). We also evaluated the freeze-drying process for NP storage in a dry state, as described previously.[19] We were able to reconstitute NPs with a similar original size after lyophilization, confirming the stability of this type of carrier to this process.

The anti-HER-2 affibody molecule was previously selected against the HER-2-ECD[20] and further modified by affinity maturation and dimerization.[14,15] The anti-HER-2 affibody is commercially available and has high binding specificity and affinity in vitro and in vivo as a targeted imaging agent.[15,21,22] Therefore, the multiple advantages of the combination of biodegradable polymeric NPs and targeting anti-HER-2 affibody molecules led to our interest in developing a targeted, controlled release drug-delivery system for cancer therapy aimed at HER-2-positive cells. Particle size and surface charge (ζ potential) of PLA-PEG-Mal NPs both with and without affibody were characterized by using laser light scattering, the ZetaPALS system, and electron microscopy (Figure 1 A). The addition of affibody molecules on the surface of the NPs did not significantly affect the size, size distribution, or surface charge of the NPs (NP $\varnothing$: 70 ± 5 nm, NP–affibody $\varnothing$: 85 ± 5 nm). The chemical conjugation of the affibody molecules at the surface of the PLA-PEG-Mal NPs was confirmed by UV imaging (Figure 1 B) and ^{1}H NMR spectroscopy in [D$_6$]DMSO (Figure 1 C). To visualize the presence of affibody molecules on the NPs, we labeled affibody molecules with the fluorescence probe Alexa fluor 532 and subsequently conjugated them to the PLA-PEG-Mal NPs at various affibody/PLA-PEG-Mal molar ratios (0, 1, 2, 5, and 20%). The NP–affibody bioconjugates were then exposed under UV light to observe their fluorescence. As shown in Figure 1 B, no fluorescence is observed from the NPs without fluorescently labeled affibody; however, the fluorescence intensity from those NPs with fluorescent affibody continuously increases with an increasing molar ratio of affibody/PLA-PEG-Mal. The ^{1}H NMR spectrum of the purified PLA-PEG–affibody in [D$_6$]DMSO shows the characteristic peaks of PLA-PEG: $\delta \sim 1.4$ ppm (–CH$_3$ of the PLA backbone), $\delta \sim 3.6$ ppm (–CH$_2$ of the PEG backbone), and $\delta \sim 5.2$ ppm (–CH of the PLA backbone) (Figure 1 B). Also evident are the characteristic peaks of the affibody molecule in the chemical shift region of $\delta = 7$–8 ppm that represents the amide bonds (NH–CO) within the affibody polypeptide molecule. The NMR results suggest successful conjugation of the affibody at the surface of PLA-PEG-Mal NPs.

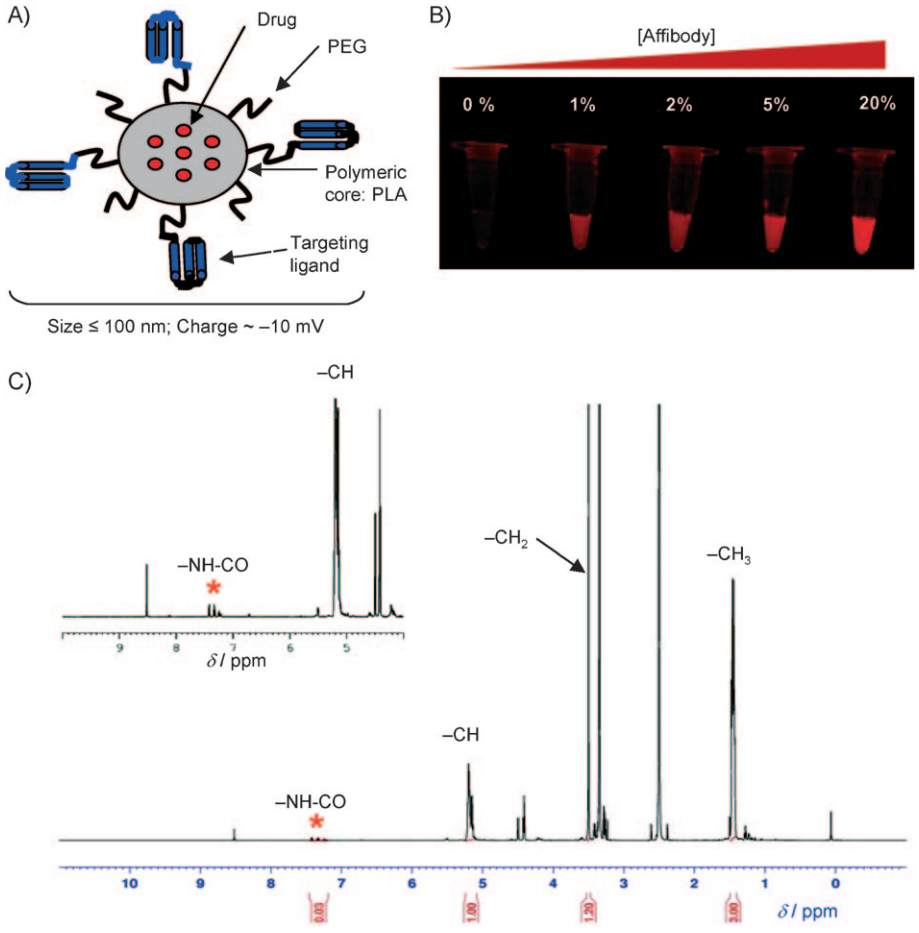

Figure 1. A) Schematic diagram of the PLA-PEG-Mal NP–affibody bioconjugates with encapsulated drug. The hydrophilic poly(ethylene glycol) (PEG) chains on the surface limit protein absorption at the hydrophobic polymeric surface to form "stealth" nanoparticles. B) Fluorescence images of fluorescent affibody (Alexa fluor 532, red) conjugated to NPs. After washing the NP–affibody bioconjugates, the fluorescence signal increases with an increased amount of fluorescent affibody (0→20% polymer/affibody molar ratio) at the NP surface, confirming the efficiency of the chemical conjugation. C) ^{1}H NMR spectrum of the PLA-PEG–affibody bioconjugates showing proton assignments to the polymer and the affibody polypeptide ($\delta = 7$–8 ppm), confirming chemical conjugation of the affibody to the polymeric NPs.

We next demonstrated the efficient binding and internalization of targeted NP–affibody bioconjugates to HER-2-positive cancer cells using three cell lines: Capan-1 (Figure 2 B1), SKBR-3 (Figure 2 B2), and SKOV-3 (Figure 2 B3). After incubating NBD dye encapsulated

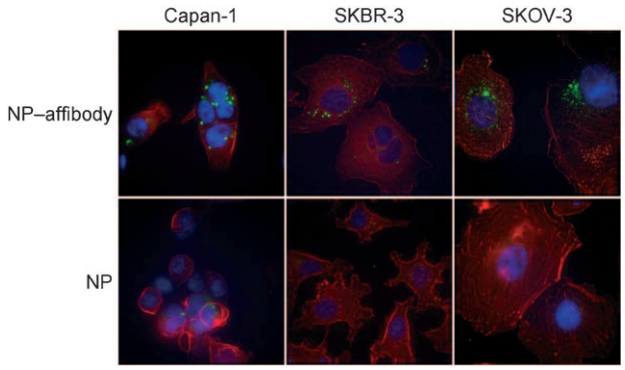

Figure 2. Fluorescence microscopy of NP–affibody bioconjugates incubated with HER-2-positive cell lines. Capan-1 cells, SKBR-3 cells, and SKOV-3 cells were grown on chamber slides and incubated in OptiMEM medium supplemented with 50 μg NBD fluorescent dye encapsulated into PLA-PEG–affibody bioconjugate NPs (shown in green) with (upper row) or without affibody (lower row) for 2 h prior to imaging with fluorescence microscopy (60× magnification). Cell nuclei and the actin cytoskeleton are stained blue (4′,6-diamidino-2-phenylindole) and red (Alexa fluor phalloidin 488), respectively. The deconvolved fluorescence images represent the mid-cross-section of the cells after wash (3×), permeabilization, and staining steps.

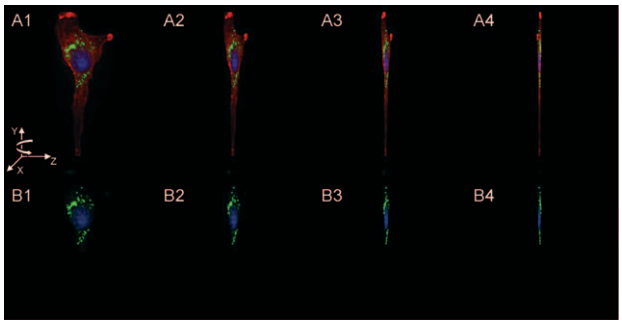

Figure 3. Combined fluorescence images (60× magnification) of a single SKBR-3 cell to reconstruct a 3D image of the cell. A1–A4 (upper row) represent the mid-cross-section of the same SKBR-3 cell rotated at 30° intervals along the *y* axis. A4 is an image of the cell rotated 90° along the *y* axis to demonstrate particles in green (NBD dye encapsulated) that are internalized inside the cell. Cell nuclei and the actin cytoskeleton are stained blue (4′,6-diamidino-2-phenylindole) and red (Alexa fluor phalloidin 488), respectively. B1–B4 (lower row) show fluorescence images of the same SKBR-3 cell as shown in the upper panel without actin cytoskeleton staining, confirming cell internalization of the NP–affibody bioconjugates.

NP–affibody bioconjugates with the cells for 2 h at 37 °C and removing excess bioconjugate, we observed a large amount of green dots in a punctuate pattern inside the targeted cells, suggesting an efficient targeting and internalization mechanism of the ~80-nm NP–affibody bioconjugates to the HER-2-positive cells. In contrast, untargeted PLA-PEG NPs were only slightly taken up by the cell lines after the same duration of incubation (Figure 2 A1, A3). To minimize the cell passage effect on the observed results, this experiment was repeated four times with different cell passages, and all of them gave the same results. We also verified the cellular localization of the NP–affibody bioconjugates using *z* axis scanning fluorescence microscopy and 3D image reconstitution. The rotated cross section of the 3D reconstitution images of a SKBR-3 cell demonstrated the internalization of targeted NP–affibody bioconjugates to the cell (Figure 3).

Orlova et al.[15] demonstrated the binding ability of anti-HER-2 affibody within 1 h using an immunofluorescence method. Our results are consistent with their findings and suggest a receptor-mediated endocytosis mechanism. Internalization through endocytosis was previously described for anti-HER-2 monoclonal antibodies[23] and is consistent with the kinetics of our targeted NPs entering the cells within 2 h.

Similarly, targeted drug delivery to integrins with RGD peptide sequences has also shown efficient binding and internalization in multiple types of cancers. In addition to efficient binding and internalization, the anti-HER-2 approach also offers greater cancer disease specificity than the RGD approach, with high affinity to HER-2 cell membrane receptors expressed in multiple cancer types.[24] We prepared drug-containing and drug-free NPs, and targeted NPs to evaluate their relative cytotoxicities using in vitro cell viability assays (MTS assays) with breast cancer (SKBR-3) and ovarian cancer cells (SKOV-3), which overexpress the HER-2 cell membrane receptors. In this study, we incubated various NP formulations with SKBR-3 and SKOV-3 cells for 2 h in OptiMEM, washed cells with phosphate-buffered saline (PBS) to remove excess NPs, and supplemented with fresh cell growth medium. We incubated the cells for a further 3 days before carrying out the MTS assay to quantify cell viability, which was normalized to that of the cells in the absence of NPs.

The results show that drug-encapsulated targeted NPs have the highest cytotoxicity toward both SKBR-3 and SKOV-3 cell lines; cell viability was 70±5% and 59±5%, respectively (Figure 4). The ANOVA test indicates that the cell viability of drug-containing targeted NPs differs significantly from that of drug-containing NPs ($p < 0.05$). In contrast, free drug and NPs without encapsulated drugs are not toxic toward either cell

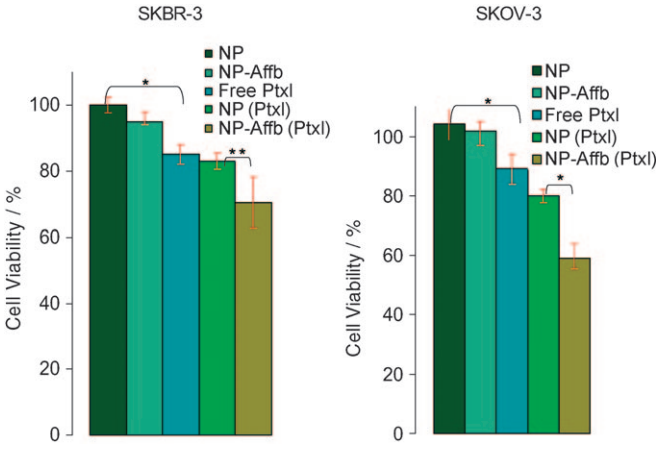

Figure 4. Cell viability (MTS) assay to evaluate the difference in toxicity between paclitaxel (PtxI) encapsulated into targeted (NP–Affb) and untargeted (NP) nanoparticles, relative to controls: free paclitaxel, and NPs with and without affibody conjugated (as indicated). In this assay, the NP formulations were incubated for 2 h, and cells were subsequently washed and incubated in cell growth media for additional 72 h before quantifying the NP formulation toxicities against two cancer cell lines expressing HER-2 (SKBR-3 and SKOV-3). ANOVA test: $*p < 0.01$, $**p < 0.05$.

line. These results are consistent with our previous studies using targeted NP–aptamer bioconjugates to deliver drugs to prostate cancer cells.[25–28] Therefore, this NP–affibody bioconjugate system has the potential for use as a biocompatible and biodegradable targeted drug delivery platform for the treatment of multiple cancer types. Furthermore, the modularity of the delivery system allows tuning of the various parameters of the bioconjugates, such as NP size, surface charge, and affibody packing density, in order to optimize the drug delivery pharmacokinetics and its targeting efficiency for optimum specific therapeutic applications.

In summary, this is, to our knowledge, the first example of a targeted controlled release NP–affibody bioconjugate for drug delivery to HER-2-positive cancer cells. Using US Food and Drug Administration (FDA)-approved polymers to form nanoparticles, we have demonstrated that the nanoparticle–affibody bioconjugates reported herein are specifically and efficiently internalized to HER-2-positive cancer cells (i.e., ovarian, breast, and pancreatic cancer), thereby providing a promising way to deliver chemotherapeutic drugs in a selective manner. This HER-2-targeted drug delivery platform can be tuned to encapsulate a variety of drug types and combinations, increase drug loading, and optimize the surface coverage of the affibody targeting ligands for specific therapeutic applications. Additional in vivo biodistribution and efficacy studies are required to further evaluate the potential of the NP–affibody bioconjugates for each therapeutic application as a systemic or locally administered drug delivery system.

Experimental Section

Nanoparticle characterization: Size (diameter) and surface charge (ζ potential) of NPs were evaluated by quasi-elastic laser light scattering (QELS) using a ZetaPALS dynamic light-scattering detector (15 mW laser, incident beam $\lambda = 676$ nm; Brookhaven Instruments, Holtsville, NY, USA). Nanoparticles (200 μg) were dispersed in solution (~2 mL), and measurements were performed in triplicate at room temperature.

Conjugation and characterization of nanoparticle–affibody bioconjugates: PLA-PEG-Mal polymeric NPs were incubated, while stirring, with anti-HER-2 affibody (15 kDa) at a molar ratio (affibody/PLA-PEG-Mal) of 5% to form a stable bioconjugate. The NP–affibody bioconjugates were purified to remove free affibody using an Amicon Ultra centrifuge (M_r size exclusion: 100 kDa). Formation of the thioether bond between PLA-PEG-Mal NPs and the affibody was subsequently characterized with ^{1}H NMR (600 MHz, Bruker Advance). Chemical attachment of the fluorescent affibody was also confirmed by UV imaging (Kodak Electrophoresis Documentation and Analysis System 120). The affibody was labeled with a red fluorescent probe (Alexa fluor 532; Invitrogen), purified, and subsequently conjugated to PLA-PEG-Mal polymeric NPs at various affibody/PLA-PEG-Mal molar ratios ranging from 0 to 20%. The purified NP–affibody bioconjugate suspensions were then imaged using a UV Kodak camera equipped with a red filter to show the visible effect of the fluorescent affibody conjugated to nonfluorescent polymeric NPs.

Uptake assays of targeted and untargeted nanoparticles: The human ovarian adenocarcinoma (SKOV-3, American-Type Culture Collection (ATCC)), human breast adenocarcinoma (SKBR-3, ATCC), and human pancreatic adenocarcinoma (Capan-1, ATCC) were the HER-2-positive cell lines used for cytotoxicity and uptake efficacy studies of the NP–affibody bioconjugates. HER-2-positive cell lines were grown in chamber slides (Cab-Tek II, eight wells; Nunc) within their growth medium [modified McCoy's 5a (ATCC) supplemented with aqueous penicillin G (100 units mL^{-1}), streptomycin (100 ug mL^{-1}), and fetal bovine serum (FBS, 10%)] to 70% confluence (50000 cells cm^{-2}) over 24 h in an incubator at 37 °C under 5% CO_2. On the day of the experiment, cells were washed with pre-warmed PBS and incubated with pre-warmed phenol-red-reduced OptiMEM media for 30 min before adding 50 μg of NPs or NP–affibody bioconjugates loaded with the same amount of green fluorescent 4-fluoro-7-nitrobenz-2-oxa-1,3-diazole (NBD) dye. NP formulations were incubated with cells for 2 h at 37 °C, washed with PBS three times, fixed with 4% paraformaldehyde, blocked for 30 min at room temperature with 1% BSA/PBS, permeabilized with 0.01% Triton-X for 3 min, counterstained with Alexa fluor phalloidin–rhodamine (cytoskeleton staining), 4′,6-diamidino-2-phenylindole (DAPI, nucleus staining), mounted in fluorescence-protecting imaging solution, and visualized with fluorescence microscopy (DeltaVision system, Olympus IX71). Digital images of green, red, and blue fluorescence were acquired along the *z* axis at intervals of 0.2 μm using a 60× oil immersion objective and DAPI, FITC, and rhodamine filters, respectively. Images were overlaid, deconvoluted, and 3D reconstruction was performed using Softwork software for acquisition and analysis.

In vitro cellular toxicity assay of paclitaxel encapsulated into targeted and untargeted NPs: SKBR-3 and SKOV-3 cells were grown in 96-well plates at concentrations leading to 70% confluence in 24 h (50000 cells cm^{-2}). Defined amounts of paclitaxel were encapsulated into targeted and untargeted nanoparticles (1% *w/w*) and incubated with cell lines (5 μg paclitaxel per well) in OptiMEM for 2 h. Next, cells were washed, and fresh media was supplemented. The cells were then allowed to grow for 72 h, and cell viability was assessed colorimetrically with MTS reagents (Invitrogen).

Acknowledgements

This work was supported by the US National Institutes of Health grant EB003647 and by a generous gift from Ms. Anne C. Gallo to Brigham and Women's Hospital toward this research.

Keywords: targeted therapy · antitumor agents · affibodies · nanoparticles · PLA-PEG copolymers

[1] O. C. Farokhzad, R. Langer, *Adv. Drug Delivery Rev.* **2006**, *58*, 1456–1459.
[2] R. Langer, *Science* **2001**, *293*, 58–59.
[3] I. Brigger, C. Dubernet, P. Couvreur, *Adv. Drug Delivery Rev.* **2002**, *54*, 631–651.
[4] M. R. Green, G. M. Manikhas, S. Orlov, B. Afanasyev, A. M. Makhson, P. Bhar, M. J. Hawkins, *Ann. Oncol.* **2006**, *17*, 1263–1268.
[5] F. M. Muggia, *J. Clin. Oncol.* **1998**, *16*, 811–812.
[6] K. J. O'Byrne, A. L. Thomas, R. A. Sharma, M. DeCatris, F. Shields, S. Beare, W. P. Steward, *Br. J. Cancer* **2002**, *87*, 15–20.
[7] T. Schluep, J. Hwang, J. Cheng, J. D. Heidel, D. W. Bartlett, B. Hollister, M. E. Davis, *Clin. Cancer Res.* **2006**, *12*, 1606–1614.
[8] K. S. Lee, H. C. Chung, S. A. Im, Y. H. Park, C. S. Kim, S. B. Kim, S. Y. Rha, M. Y. Lee, J. Ro, *Breast Cancer Res. Treat* **2008**, *108*, 241–250.
[9] F. Alexis, J. W. Rhee, J. P. Richie, A. F. Radovic-Moreno, R. Langer, O. C. Farokhzad, *Urol. Oncol.* **2008**, *26*, 74–85.
[10] E. M. Pridgen, R. Langer, O. C. Farokhzad, *Nanomedicine* **2007**, *2*, 669–680.

[11] L. E. van Vlerken, M. M. Amiji, *Expert Opin. Drug Delivery* **2006**, *3*, 205–216.
[12] M. V. Pimm, *Crit. Rev. Ther. Drug Carrier Syst.* **1988**, *5*, 189–227.
[13] M. Dowsett, C. Harper-Wynne, I. Boeddinghaus, J. Salter, M. Hills, M. Dixon, S. Ebbs, G. Gui, N. Sacks, I. Smith, *Cancer Res.* **2001**, *61*, 8452–8458.
[14] K. Kimura, T. Sawada, M. Komatsu, M. Inoue, K. Muguruma, T. Nishihara, Y. Yamashita, N. Yamada, M. Ohira, K. Hirakawa, *Clin. Cancer Res.* **2006**, *12*, 4925–4932.
[15] A. Orlova, M. Magnusson, T. L. Eriksson, M. Nilsson, B. Larsson, I. Hoiden-Guthenberg, C. Widstrom, J. Carlsson, V. Tolmachev, S. Stahl, F. Y. Nilsson, *Cancer Res.* **2006**, *66*, 4339–4348.
[16] M. Vittaz, D. Bazile, G. Spenlehauer, T. Verrecchia, M. Veillard, F. Puisieux, D. Labarre, *Biomaterials* **1996**, *17*, 1575–1581.
[17] B. Romberg, C. Oussoren, C. J. Snel, W. E. Hennink, G. Storm, *Pharm. Res.* **2007**, *24*, 2394–3401.
[18] B. Romberg, W. E. Hennink, G. Storm, *Pharm. Res.* **2008**, *25*, 55–71.
[19] J. Cheng, B. A. Teply, I. Sherifi, J. Sung, G. Luther, F. X. Gu, E. Levy-Nissenbaum, A. F. Radovic-Moreno, R. Langer, O. C. Farokhzad, *Biomaterials* **2007**, *28*, 869–876.
[20] M. Friedman, E. Nordberg, I. Hoiden-Guthenberg, H. Brismar, G. P. Adams, F. Y. Nilsson, J. Carlsson, S. Stahl, *Protein Eng. Des. Sel.* **2007**, *20*, 189–199.
[21] A. Orlova, V. Tolmachev, R. Pehrson, M. Lindborg, T. Tran, M. Sandström, F. Y. Nilsson, A. Wennborg, L. Abrahmsén, J. Feldwisch, *Cancer Res.* **2007**, *67*, 2178–2186.
[22] V. Tolmachev, A. Orlova, F. Y. Nilsson, J. Feldwisch, A. Wennborg, L. Abrahmsen, *Expert Opin. Biol. Ther.* **2007**, *7*, 555–568.
[23] L. A. Maier, F. J. Xu, S. Hester, C. M. Boyer, S. McKenzie, A. M. Bruskin, Y. Argon, R. C. Bast, Jr., *Cancer Res.* **1991**, *51*, 5361–5369.
[24] E. Ruoslahti, *Annu. Rev. Cell Dev. Biol.* **1996**, *12*, 697–715.
[25] L. Zhang, A. F. Radovic-Moreno, F. Alexis, F. X. Gu, P. A. Basto, V. Bagalkot, S. Jon, R. S. Langer, O. C. Farokhzad, *ChemMedChem* **2007**, *2*, 1268–1271.
[26] O. C. Farokhzad, J. Cheng, B. A. Teply, I. Sherifi, S. Jon, P. W. Kantoff, J. P. Richie, R. Langer, *Proc. Natl. Acad. Sci. USA* **2006**, *103*, 6315–6320.
[27] O. C. Farokhzad, S. Jon, A. Khademhosseini, T. N. Tran, D. A. Lavan, R. Langer, *Cancer Res.* **2004**, *64*, 7668–7672.
[28] F. Gu, L. Zhang, B. A. Teply, N. Mann, A. Wang, A. F. Radovic-Moreno, R. Langer, O. C. Farokhzad, *Proc. Natl. Acad. Sci. USA* **2008**, *105*, 2586–2591.

Received: April 17, 2008
Revised: September 19, 2008
Published online on November 14, 2008

